Ligand Variation in the Transferrin Family: The Crystal Structure of the H249Q Mutant of the Human Transferrin N-lobe As a Model for Iron Binding in Insect Transferrins[†,‡]

Heather M. Baker,[§] Anne B. Mason,[||] Qing-Yu He,[||] Ross T. A. MacGillivray,[⊥] and Edward N. Baker*[,§,#]

School of Biological Sciences and Department of Chemistry, University of Auckland, Auckland, New Zealand, and Department of Biochemistry, University of Vermont, Burlington, Vermont 05405, and Department of Biochemistry and Molecular Biology, University of British Columbia, Vancouver, British Columbia V6T 1Z3, Canada

Received May 3, 2001; Revised Manuscript Received August 10, 2001

ABSTRACT: Proteins of the transferrin (Tf) family play a central role in iron homeostasis in vertebrates. In vertebrate Tfs, the four iron-binding ligands, 1 Asp, 2 Tyr, and 1 His, are invariant in both lobes of these bilobal proteins. In contrast, there are striking variations in the Tfs that have been characterized from insect species; in three of them, sequence changes in the C-lobe binding site render it nonfunctional, and in all of them the His ligand in the N-lobe site is changed to Gln. Surprisingly, mutagenesis of the histidine ligand, His249, to glutamine in the N-lobe half-molecule of human Tf (hTf/2N) shows that iron binding is destabilized and suggests that Gln249 does not bind to iron. We have determined the crystal structure of the H249Q mutant of hTf/2N and refined it at 1.85 Å resolution ($R = 0.221$, $R_{free} = 0.246$). The structure reveals that Gln249 does coordinate to iron, albeit with a lengthened Fe−Oϵ1 bond of 2.34 Å. In every other respect, the protein structure is unchanged from wild-type. Examination of insect Tf sequences shows that the K206···K296 dilysine pair, which aids iron release from the N-lobes of vertebrate Tfs, is not present in the insect proteins. We conclude that substitution of Gln for His does destabilize iron binding, but in the insect Tfs this is compensated by the loss of the dilysine interaction. The combination of a His ligand with the dilysine pair in vertebrate Tfs may have been a later evolutionary development that gives more sophisticated pH-mediated control of iron release from the N-lobe of transferrins.

The transferrins (Tfs)[1] are a family of proteins that are widely distributed in vertebrates, where they perform essential iron-binding functions (*1*, *2*). Serum transferrin (Tf) has the role of transporting iron in the bloodstream, delivering it to cells by a process of receptor-mediated endocytosis (*3*, *4*). Its closely related homologue lactoferrin (Lf), with ∼60% sequence identity, occurs in many bodily secretions where it serves to control iron levels and so afford bacteriostatic and antioxidant protection. Ovotransferrin (oTf), present in avian egg white, provides similar protection.

The vertebrate Tfs are 80 kDa glycoproteins whose amino acid sequences have a 2-fold internal repeat (∼40% sequence identity between their N-terminal and C-terminal halves). Correspondingly, crystallographic studies show that each protein is folded into two homologous lobes (their N- and C-lobes), with each lobe further divided into two domains that enclose an iron binding site between them (*2*). The iron binding sites are highly conserved; in each protein, the same group of ligands is found in both the N-lobe and C-lobe sites (*5*−*7*). These invariably comprise two tyrosines, one aspartate and one histidine (Asp63, Tyr95, Tyr188, and His249 in the N-lobe of human Tf), together with two oxygen atoms from the bidentate carbonate ion.

Intriguing variations are, however, found in some more evolutionarily distant members of the transferrin family. These are the transferrins that have been characterized from a number of insect species, including the cockroach *Blaberus discoidalis* (*8*), the sphinx moth *Manduca sexta* (*9*), the mosquito *Aedes aegypti* (*10*), the flesh fly *Sarcophaga peregrina* (*11*), and the silkworm *Bombyx mori* (*12*). These proteins have significant structural and functional differences from their vertebrate counterparts. Sequence identity between the insect and vertebrate Tfs is only 25−30%, but of most significance to likely functions dependent on iron binding, and to iron homeostasis in insects, there are striking changes in their presumed iron binding sites. In four out of five insect Tfs, most of the ligands in the C-lobe are missing, and in these proteins, as in the human melanotransferrin (*13*), the C-lobe cannot bind iron. Furthermore, in all of the insect proteins, the His ligand in the N-lobe is changed, in four cases to Gln and in the fifth to Thr.

[†] Supported by grants from the U.S. Public Health Service (RO1-HD20859 to E.N.B.; RO1-DK21739 to A.B.M.), the Marsden Fund of New Zealand, the Health Research Council of New Zealand, and the Wellcome Trust (U.K.) through a Major Equipment Grant.

[‡] Atomic coordinates have been deposited with the Protein Data Bank with accession code 1jqf.

* To whom correspondence should be addressed. Phone: (+64) 9-373-7599. Fax: (+64) 9-373-7619. E-mail: ted.baker@auckland.ac.nz.

[§] School of Biological Sciences, University of Auckland.

[||] University of Vermont.

[⊥] University of British Columbia.

[#] Department of Chemistry, University of Auckland.

[1] Abbreviations: Tf, transferrin; Lf, lactoferrin; hTf/2N, recombinant N-terminal half-molecule of human transferrin, residues 1−337; mutants of hTf/2N are designated by the wild-type amino acid residue, the sequence number, and the amino acid to which the residue was mutated, e.g., K206A; BHK cells, baby hamster kidney cells; PEG, poly(ethylene glycol); rms, root-mean-square.

10.1021/bi010907p CCC: $20.00
Published on Web 09/06/2001

We have previously shown, in a mutational study of the His ligand in the N-lobe half-molecule of human Tf, hTf/2N, that mutation of His249 to Gln significantly destabilizes iron binding; the protein releases iron more than 1 pH unit higher than wild-type, and in kinetic studies releases iron 10^4 times faster (*14*). The properties of the H249Q mutant also mirror those of the H249A mutant, in which residue 249 (Ala) cannot bind to iron, leading to questions as to whether the Gln residue in H249Q binds iron at all (*14*, *15*).

What, then, are the implications for the insect Tfs? To have a role in iron transport or to function in a protective role by iron sequestration, as proposed, for example, for the mosquito Tf, which is an acute phase protein that is upregulated upon infection (*10*), at least one site must have strong iron binding ability. The cockroach Tf has normal iron-binding properties (*16*), but this is the one insect Tf that has an unchanged, functional C-lobe binding site. The other insect Tfs lack a functional C-lobe site, and the presence of Gln (and in one case Thr) in their N-lobe sites raises doubts about their iron binding ability, by analogy with the H249Q hTf/2N mutant described above.

In the absence of a crystal structure of any of the insect proteins, we have addressed these questions by determining the crystal structure of the H249Q mutant of hTf/2N. We find that the Gln ligand is indeed coordinated to the iron atom, albeit with a somewhat longer bond than is made by His, and further conclude, by correlation with functional and amino acid sequence data, that the weakened coordination of Gln is in the insect Tfs counterbalanced by the absence of a critical dilysine interaction that is a feature of vertebrate Tfs.

MATERIALS AND METHODS

Protein Production, Purification, and Crystallization. The mutation of His249 to Gln was introduced into the gene for the N-terminal half-molecule of human transferrin (residues 1−337 of the native protein) using a PCR-based procedure (*14*). The H249Q protein was then expressed in baby hamster kidney (BHK) cells, using the pNUT vector, and purified from the tissue culture medium (*14*). Ferric nitrilotriacetate was added to the tissue culture medium during this isolation and the protein was thus obtained in its fully iron-saturated form. To ensure that a homogeneous Fe(III)/H249Q/carbonate complex was used for crystallization, however, the protein was then exchanged into Hepes buffer containing 0.1 M bicarbonate, at pH 7.4. The resulting orange complex, with a visible absorption maximum λ_{max} at 463 nm, was used for crystallization.

Crystals were grown at room temperature in hanging drops prepared using 2 μL of protein solution (35 mg mL^{-1} of H249Q) and 2 μL of reservoir solution (0.1 M potassium acetate, pH 7.4, containing 20−25% PEG 3350). Diffraction-quality crystals were obtained by a micro-seeding procedure (*17*) that used crushed crystals of the wild-type hTf/2N to give the initial seeds. High-quality red, blocklike crystals, diffracting to better than 2.0 Å, grew overnight. These crystals were orthorhombic, space group $P2_12_12_1$, with one protein molecule in the asymmetric unit, and cell dimensions $a = 44.2$, $b = 57.2$, $c = 135.75$ Å. The crystals are closely isomorphous with the wild-type protein Form 1 crystals (*18*).

Data Collection and Structure Determination. X-ray diffraction data were collected from flash-frozen crystals at 110 K after transfer of the crystals to a cryoprotectant comprising 0.1 M potassium acetate, pH 7.4, with 35% PEG 3350. Data were collected with CuKα radiation, wavelength 1.54 Å, using a Rigaku RU-300 rotating anode generator equipped with double focusing mirrors and a Mar345 imaging plate detector. Reflection data were indexed and integrated using DENZO (*19*) and scaled and merged using programs from the CCP4 suite (*20*). A data set of 96% completeness to 1.85 Å resolution was obtained (see Table 1 for full statistics).

Table 1: H249Q Data Collection, Refinement, and Model Statistics

data collection[a]	
maximum resolution (Å)	1.85
unique reflections	30 081
redundancy	4.6 (3.2)
completeness (%)	99.4 (96.5)
merging *R* factor	0.087 (0.395)
mean I/σ	17.0 (2.9)
refinement	
resolution range (Å)	30.0−1.85
R-factor (no. of reflections)	0.221 (27 447)
R_{free} (no. of reflections)	0.246 (1426)
rms deviation bond lengths (Å)	0.005
rms deviation bond angles (degrees)	1.25
model	
no. of protein atoms	2546
ions	1 Fe^{3+}, 1 CO_3^{2-}, 1 K^+
no. of water molecules	191

[a] Figures in parentheses are for the outermost resolution shell, 1.92−1.85 Å.

An initial model for the structure was obtained from the isormorphous 1.6 Å resolution wild-type hTf/2N structure (*18*), Form 1, PDB entry code 1A8E, after removal of all water molecules and the Fe^{3+} and CO_3^{2-} ions and truncation of residue 249 to Ala. Rigid-body refinement, first as the whole molecule, then as two domains, was carried out with CNS (*21*), followed by simulated annealing between 10 000 and 100 K. SIGMAA-weighted ($2mF_o - DF_c$) and ($mF_o - DF_c$) difference electron density maps were calculated and were interpreted using the TURBO FRODO graphics package (*22*) on a Silicon Graphics workstation. The positions of the carbonate and ferric ions, and the Gln side chain at position 249 (Figure 1), were clearly apparent and were added to the model. In further cycles of refinement with CNS, water molecules were added automatically and were then visually inspected in SIGMAA-weighted ($2mF_o - DF_c$) and (mF_o - DF_c) maps. Only those sites that had good spherical electron density, reasonable *B*-factors, and hydrogen bond partners with appropriate geometry were retained in the model at each stage. The conformations of the Gln249 side chain and its neighbors were checked at several stages during refinement, with omit maps, and found to have excellent electron density (Figure 1). One solvent molecule was assigned as a potassium ion, as its environment suggested a cation and its *B*-factor when refined as water was 1 Å^2; when the atom was refined as K^+ the *B*-factor assumed a much more reasonable value of 18.0 Å^2. The final values for *R* and R_{free} were 0.221 and 0.246 for all data in the resolution range 30.0 to 1.85 Å, with approximately 5% of reflections used in the free *R* calculation. Full refinement and model statistics are given in Table 1.

Final Model. The final model comprises 2546 protein atoms, one Fe^{3+} ion, one K^+ ion, one CO_3^{2-} ion, and 191

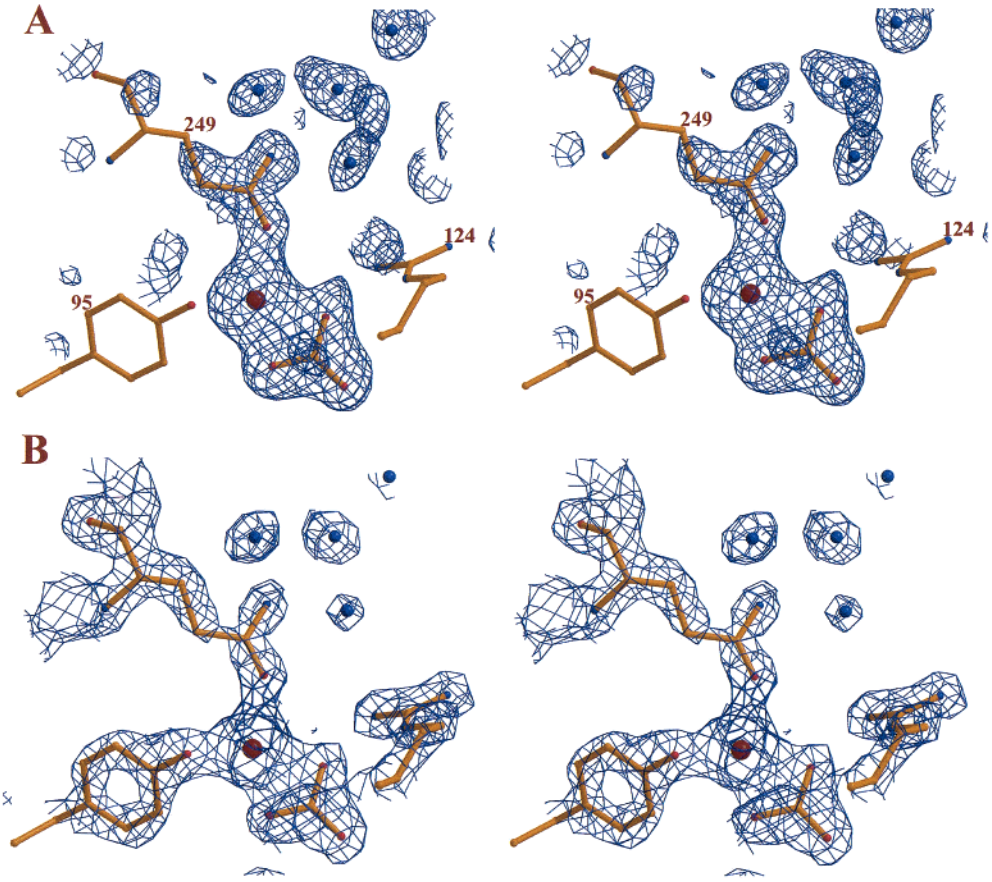

FIGURE 1: Stereoviews of the electron density for the side chain of Gln249 and surrounding structure. (a) Difference electron density, contoured at 3σ, for the Gln249 side chain, the Fe^{3+} and CO_3^{2-} ions and nearby water molecules, prior to their inclusion in the model. (b) The final $2F_o - F_c$ map contoured at 2σ.

water molecules. The protein model comprises 329 of 337 residues, as no density could be found for residues 1−2 and 332−337. The rest of the model conforms well with standard geometry, with 86% of residues in the most favored regions of the Ramachandran plot as defined by the program PROCHECK (*23*).

Other Methods. Potential hydrogen bonds were identified using the criteria of Baker and Hubbard (*24*). Figures were drawn using MOLSCRIPT (*25*), rendered with RASTER3D (*26*).

RESULTS AND DISCUSSION

Protein Structure. The polypeptide folding for H249Q is unchanged from that of wild-type hTf/2N (*18*) and other site-specific mutants (*15*, *17*). Superposition of the whole polypeptide chain on to wild-type hTf/2N gives an overall rms difference in atomic positions of 0.32 Å for 324 Cα atoms (residues 4−327). Superpositions of the individual domains give almost identical rms differences of 0.34 Å for domain 1 (Cα atoms of residues 4−94 and 249−327) and 0.23 Å for domain 2 (residues 95−248). This implies that there is no change in domain orientations associated with the H249Q mutation, as is also shown by the fact that when the N2 domains of H249Q and wild-type are superimposed, less than a 1° rotation is required to then superimpose the N1 domains. The single K^+ ion that was identified during refinement does not appear to be present in wild-type hTf/2N, but a K^+ ion was found at the same site in another mutant, K206A, bound in a surface loop to the peptide oxygen atoms of residues 151, 152, and 154, the side-chain amide oxygen of Gln169, and a water molecule. This K^+ ion presumably originates from the use of potassium acetate as a buffer for crystallization of H249Q (but not for wild-type).

At the mutation site, Gln249 is coordinated to the iron atom through its side-chain amide oxygen atom with an Fe−Oε1 bond of 2.34 Å. The rest of the iron coordination sphere is essentially unchanged from wild-type with respect to both bond lengths and angles (Table 2). The similarity in the geometry of the Fe−Tyr interactions is reflected in the very similar λ_{max} values for the visible charge-transfer absorption band, 463 nm for H249Q, and 472 nm for wild-type (*14*). Sterically, the side chains of Gln and His are quite similar, with the Oε1 atom of Gln249 displaced only 1.0 Å from the position of the His249 Nε2 atom in wild-type and Nε2 of Gln249 displaced 0.9 Å from the position of His249 Nδ1 in wild-type (Figure 2). The plane of the Gln249 amide group also coincides with that of the His249 imidazole ring. The result is that a lone pair of electrons on Gln249 Oε1 is directed toward the iron atom with an angle Cδ-Oε1-Fe of 144°, close to the optimal 120°. This implies a favorable bonding interaction, albeit rather longer than the Fe−His bond in wild-type.

The small displacement of the Gln Oε1 atom relative to the His Nε2 atom does, however, change the Fe−ligand bond angles associated with this atom (Table 2) enough to change some of the spectroscopic properties of the iron site. The EPR spectra of both the H249Q and H249A mutants of hTf/

Table 2: Iron Coordination Geometry[a]

	H249Q	wt hTf/2N[b]
metal−ligand bond lengths (Å)		
Fe−O$\delta 1_{63}$	2.11	2.02
Fe−Oη_{95}	2.00	1.99
Fe−Oη_{188}	1.88	1.90
Fe−O$\epsilon 1_{249}$	**2.34**	**2.10**[c]
Fe−O1 (CO_3^{2-})	2.20	2.06
Fe−O2 (CO_3^{2-})	2.18	2.24
ligand−metal−ligand bond angles (deg)		
O$\delta 1_{63}$−Fe−Oη_{95}	85	85
O$\delta 1_{63}$−Fe−Oη_{188}	177	178
O$\delta 1_{63}$−Fe−O$\epsilon 1_{249}$	**88**	**87**[c]
O$\delta 1_{63}$−Fe−O1	85	82
O$\delta 1_{63}$−Fe−O2	88	90
Oη_{95}−Fe− Oη_{188}	94	96
Oη_{95}−Fe− O$\epsilon 1_{249}$	**106**	**92**[c]
Oη_{95}−Fe−O1	94	93
Oη_{95}−Fe−O2	156	155
Oη_{188}−Fe− O$\epsilon 1_{249}$	**89**	**91**[c]
Oη_{188}−Fe−O1	98	100
Oη_{188}−Fe−O2	93	90
O$\epsilon 1_{249}$−Fe−O1	**158**	**168**[c]
O$\epsilon 1_{249}$−Fe−O2	**96**	**113**[c]
O1−Fe−O2	63	62

[a] Figures in bold highlight bonds and angles for residue 249. [b] Data for wild-type hTf/2N from ref 18. [c] His249 Nϵ2 for wild-type hTf/2N.

2N are changed from the split rhombic signal characteristic of native transferrins to a pure rhombic signal (*14*). This change had previously been taken as an indication of the loss of one ligand, but we now attribute it to the small but significant rearrangement of the iron coordination geometry.

The Nϵ2 atom of Gln249 also hydrogen bonds to a water molecule (OW767) that corresponds precisely (only 0.1 Å displacement) with the position of a water molecule (OW341) hydrogen bonded to His249 Nδ1 in wild-type. Gln249 Nϵ2, with two available protons, also hydrogen bonds to a second water molecule (OW903) but this, too, corresponds to a water molecule (OW460) present in the wild-type structure. In fact, of 10 water molecules within 8 Å of Gln249, nine of them correspond with waters present in the wild-type structure, with an average positional difference of only 0.3 Å. The hydrogen-bonded dilysine interaction between Lys206 and Lys296 that plays a key role in iron release from hTf/2N (*17*, *27*−*29*) is also present in the mutant; the distance 206Nζ···296Nζ is 3.04 Å in wild-type and 3.05 Å in H249Q.

A strong and important conclusion from these structural comparisons is therefore that the substitution of Gln for His at this position (a) changes the iron coordination by substituting an amide oxygen ligand for an imidazole nitrogen, with a somewhat longer Fe−ligand bond (Table 2), but (b) produces no change in the surrounding protein structure, even in the positions of bound solvent molecules.

Effects of Ligand Substitution on Iron Binding by H249Q. In our previous functional studies of the H249Q protein, it was found to have strikingly altered properties, both in the kinetics of iron release to chelators and in the acid stability of iron binding (*14*). Iron release from H249Q to chelators occurred 10^4 times faster than wild-type, and the pH profile of iron release showed that iron was released from H249Q over the pH range 6.5 to 5.5, about 1 pH unit higher than wild-type. Most significantly, the iron release properties of H249Q were almost identical to those of H249A, leading to the natural conclusion that Gln249 was not bound to iron in H249Q. The present crystal structure, however, shows that this is not the case.

The more facile iron release from the H249Q mutant must reflect weaker iron binding, since the Gln amide side chain is not protonated in the pH range in question, and we see no mechanism by which the substitution could change the kinetic mechanism of iron release. Thus, we conclude that Gln is a significantly weaker ligand than His for Fe(III) in the transferrin binding site. This presumably arises because the amide oxygen is a weaker electron donor than imidazole nitrogen and does not allow for significant π-interaction. The weakened interaction is also reflected in the longer bond length.

We can now also reassess other mutational studies in the light of the Gln coordination found for H249Q. The mutation of His249 to Ala gives a protein (H249A) with iron binding and iron release properties very similar to those of H249Q (*14*). Since there is no side chain group to coordinate iron, the most likely explanation for this similarity is that a water molecule coordinates instead, probably hydrogen bonded to one or more protein groups as well. The similarity in EPR spectra for H249Q and H249A implies that the geometry must also be quite similar. In contrast, the substitution of Glu for His gives almost identical iron release properties to wild-type, but here the situation is more complex; the weaker bonding by the Glu ligand is counterbalanced by a gain in stability as the "dilysine pair" (Lys206−Lys296) interaction is broken to allow Lys296 to interact with Glu249 (*15*).

Implications for Insect Transferrins. The difference between vertebrate transferrins and insect transferrins at position 249 (human Tf numbering) is remarkable; His249 is conserved in all vertebrate Tfs whereas almost all insect Tfs have Gln (the only exception being Thr). The present work shows that Gln can act as a ligand, but the functional implications are contradictory. From iron release studies on H249Q, iron binding should be significantly weakened by the substitution, yet the pH profile of iron release for the cockroach Tf (the only insect protein for which such data are available) appears normal (*16*).

Two explanations seem possible. First, since the cockroach Tf, unlike the other insect Tfs, has two functional binding sites, it is possible that iron binding in the C-lobe imparts some additional stability to the N-lobe, as is the case for lactoferrin (*30*, *31*). A more likely explanation, however, is suggested by further examination of the sequences (Table 3). None of the insect proteins appears to have an intact dilysine pair, such as is found in the N-lobes of vertebrate Tfs (*17*, *27*, *29*, *32*). Lys206 is conserved, as are the residues adjacent to it, but sequence alignments give no match to Lys296, which appears to be changed to a hydrophobic residue (Leu, Val, or Ile), in a part of the sequence that is radically changed in the insect proteins. The Gln substitution, giving weakened iron binding, should then be compensated by the loss of the dilysine interaction, giving enhanced iron retention, a situation very similar to that found for the H249E mutant of hTf/2N (*15*).

The biological roles of the insect Tfs are not clearly established. In the silkworm and the mosquito, Tf expression is upregulated in response to bacterial invasion or injection of bacteria, leading to speculation that Tf in these organisms deprives pathogens of iron (*10*), as has been suggested for

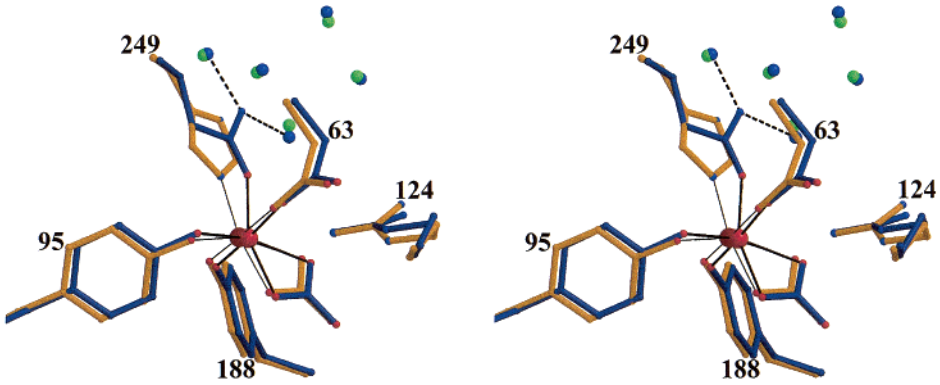

FIGURE 2: Stereoview of the iron sites of wild-type hTf/2N (gold, with dark red iron atom) and H249Q (blue, with light red iron atom), after superposition on the basis of their protein structures. The slight displacement of the coordinating Gln249 Oϵ1 atom relative to the His249 Nϵ2 atom, and the striking correspondence of the surrounding structure can be seen. Hydrogen bonds made by the Gln249 Nϵ2 atom are shown with broken lines.

Table 3: Sequence Comparisons[a]—Vertebrate and Insect Tfs[b]

Protein[c]	206															249											296			
hTf	A	F	V	**K**	H	S	T	.	.	.	A	Q	V	P	S	**H**	T	V	V	A	.	.	.	D	L	L	F	**K**	D	S	A
pTf	A	F	V	**K**	H	S	T	.	.	.	A	Q	V	P	S	**H**	A	V	V	A	.	.	.	D	L	L	F	**K**	D	S	A
eTf	A	F	V	**K**	H	S	T	.	.	.	A	S	I	P	S	**H**	A	V	V	A	.	.	.	D	L	L	F	**K**	D	S	A
rTf	A	F	V	**K**	Q	E	T	.	.	.	A	R	V	P	S	**H**	A	V	V	A	.	.	.	D	L	L	F	**K**	D	S	A
oTf	A	F	V	**K**	H	T	T	.	.	.	A	R	V	A	A	**H**	A	V	V	A	.	.	.	D	L	L	F	**K**	D	S	A
msTf	A	F	T	**K**	V	I	F	.	.	.	A	A	R	P	W	Q	G	L	I	G	.	.	.	K	V	L	G	L	S	E	K
bdTf	A	W	T	**K**	V	Y	Y	.	.	.	A	A	R	P	W	Q	G	Y	M	A	.	.	.	K	V	L	D	L	N	N	K
aaTf	A	F	T	**K**	V	I	Y	.	.	.	A	Q	R	P	W	Q	G	Y	M	G	.	.	.	L	K	M	W	V	D	R	K
bmTf	A	F	T	**K**	V	I	F	.	.	.	A	A	R	P	W	Q	G	L	I	G	.	.	.	K	V	L	G	L	S	D	K
spTf	A		T	**K**	V	Q	F	.	.	.	A	Q	R	P	W	T	G	Y	I	S	.	.	.	S	H	L	L	I	N	P	N

[a] Sequence alignments around the histidine ligand, His249, and the dilysine pair residues, Lys206 and Lys296 (human Tf numbering). [b] Sequences for vertebrate Tfs from Baldwin (*33*), and for insect Tfs from refs *8*−*12*. Alignment of vertebrate and insect sequences taken from Yoshiga et al. (*10*). [c] Proteins are: hTf, human Tf; pTf, porcine Tf; eTf, equine Tf; rTf, rabbit Tf; oTf, hen ovoTf; msTf, *Manduca sexta* Tf; bdTf, *Blaberus discoidalis* Tf; aaTf, *Aedus aegypti* Tf; bmTf, *Bombyx mori* Tf; spTf, *Sarcophaga peregrina* Tf.

lactoferrin in exocrine secretions or ovotransferrin in egg white (*32*). That is, iron must be strongly retained under the physiological conditions that apply. In the cockroach and flesh fly, however, and possibly in other insects, it has been suggested that Tf is required to ensure adequate availability of iron to the eggs and so sustain embryonic growth (*8*, *11*). For this function, it may be advantageous for iron release to occur reasonably readily, depending on whether specific receptors exist to facilitate iron delivery. From our studies on H249Q, we speculate that the presence of Gln as a ligand, with its weakened iron binding, makes an iron delivery role more likely.

The characteristic difference between vertebrate Tfs, with their His ligand and dilysine pair, and the insect Tfs, with their weaker Gln or Thr ligand and no dilysine pair, suggests an evolutionary differentiation of their functional requirements. We suggest that the combination, in the N-lobes of vertebrate Tfs, of the His ligand and the dilysine pair, both able to be protonated at lowered pH, is a later evolutionary development that allows a more sophisticated pH-dependent mechanism for the control of iron release.

CONCLUSIONS

We have shown that Gln can replace His as an iron ligand in transferrins, but that it binds to iron significantly more weakly. In the canonical iron binding site in vertebrate Tfs, three negatively charged ligands, two Tyr and one Asp, balance the charge of the Fe^{3+} ion, leaving the neutral His ligand to maintain the electroneutrality of the site (*2*). Gln is similarly neutral, but is a poorer electron donor, and its substitution for His enhances iron release. The overall control of iron binding in transferrins depends, however, on second shell residues, which can significantly perturb the ease of iron release (*29*, *34*). Thus, in the insect Tfs the substitution of Gln for His might be expected to impair iron binding ability, to the detriment of function; this is counterbalanced, however, by the accompanying absence of the dilysine interaction found in vertebrate Tfs. We suggest that the presence of the stronger His ligand, together with the dilysine pair, may represent a later evolutionary development in the N-lobes of vertebrate Tfs to couple iron release more strongly to physiological pH.

ACKNOWLEDGMENT

We gratefully acknowledge Drs. Didier Nurizzo and Clyde Smith for helpful discussion during data processing and refinement.

REFERENCES

1. Brock, J. H. (1985) in *Metalloproteins* (Harrison, P., Ed.) pp 183−262, MacMillan, London.
2. Baker, E. N. (1994) *Adv. Inorg. Chem. 41*, 389−463.
3. Klausner, R. D., Ashwell, J. V., Van Renswoude, J. B., Harford, J., and Bridges, K. (1983) *Proc. Natl. Acad. Sci. U.S.A. 80*, 2263−2267.
4. Aisen, P. (1998) *Metal Ions Biol. Syst. 35*, 585−631.

5. Bailey, S., Evans, R. W., Garratt, R. C., Gorinsky, B., Hasnain, S., Horsburgh, C., Jhoti, H., Lindley, P. F., Mydin, A., Sarra, R., and Watson, J. L. (1988) *Biochemistry 27*, 5804−5812.
6. Anderson, B. F., Baker, H. M., Norris, G. E., Rice, D. W., and Baker, E. N. (1989) *J. Mol. Biol. 209*, 711−734.
7. Kurokawa, H., Mikami, B., and Hirose, M. (1995) *J. Mol. Biol. 254*, 196−207.
8. Jamroz, R. C., Gasdaska, J. R., Bradfield, J. Y., and Law, J. H. (1993) *Proc. Natl. Acad. Sci. U.S.A. 90*, 1320−1324.
9. Bartfeld, N. S., and Law, J. H. (1990) *J. Biol. Chem. 265*, 21684−21691.
10. Yoshiga, T., Hernandez, V. P., Fallon, A. M., and Law, J. H. (1997) *Proc. Natl. Acad. Sci. U.S.A. 94*, 12337−12342.
11. Kurama, T., Kurata, S., and Natori, S. (1995) *Eur. J. Biochem. 228*, 229−235.
12. Yun, E. Y., Kang, S. W., Hwang, J. S., Goo, T. W., Kim, S. H., Jin, B. R., Kwon, O.-Y., and Kim, K. Y. (1999) *Biol. Chem. 380*, 1455−1459.
13. Baker, E. N., Baker, H. M., Smith, C. A., Stebbins, M. R., Kahn, M., Hellstrom, K. E., and Hellstrom, I. (1992) *FEBS Lett. 298*, 215−218.
14. He, Q.-Y., Mason, A. B., Pakdaman, R., Chasteen, N. D., Dixon, B. K., Tam, B. M., Nguyen, V., MacGillivray, R. T. A., and Woodworth, R. C. (2000) *Biochemistry 39*, 1205−1210.
15. MacGillivray, R. T. A., Bewley, M. C., Smith, C. A., He, Q.-Y., Mason, A. B., Woodworth, R. C., and Baker, E. N. (2000) *Biochemistry 39*, 1211−1216.
16. Gasdaska, J. R., Law, J. H., Bender, C. J., and Aisen, P. (1996) *J. Inorg. Biochem. 64*, 247−258.
17. Nurizzo, D., Baker, H. M., He, Q.-Y., MacGillivray, R. T. A., Mason, A. B., Woodworth, R. C., and Baker, E. N. (2001) *Biochemistry 40*, 1616−1623.
18. MacGillivray, R. T. A., Moore, S. A., Chen, J., Anderson, B. F., Baker, H., Luo, Y., Bewley, M., Smith, C. A., Murphy, M. E., Wang, Y., Mason, A. B., Woodworth, R. C., Brayer, G., and Baker, E. (1998) *Biochemistry 37*, 7919−7928.
19. Otwinowski, Z., and Minor, W. (1997) *Methods Enzymol. 276*, 307−326.
20. CCP4 (Collaborative Computational Project, N. (1994) *Acta Crystallogr., Sect. D 50*, 760−763.
21. Brunger, A. T., Adams, P. D., Clore, G. M., DeLano, W. L., Gros, P., Grosse-Kunstleve, R. W., Jiang, J. S., Kuszewski, J., Nilges, M., Pannu, N. S., Read, R. J., Rice, L. M., Simonson, T., and Warren, G. L. (1998) *Acta Crystallogr., Sect. D 54*, 905−921.
22. Cambillau, C., Roussel, A., Inisan, A.-G., and Knoops-Mouthuy, E. (1996) Bio-Graphics, AFMB-CNRS, Marseille, France.
23. Laskowski, R., MacArthur, M., Moss, D., and Thornton, J. M. (1993) *J. Appl. Crystallogr. 26*, 283−291.
24. Baker, E. N., and Hubbard, R. E. (1984) *Prog. Biophys. Mol. Biol. 44*, 97−179.
25. Kraulis, P. J. (1991) *J. Appl. Crystallogr. 24*, 946−950.
26. Merritt, E. A., and Murphy, W. F. (1994) *Acta Crystallogr., Sect. D 50*, 869−873.
27. Dewan, J. C., Mikami, B., Hirose, M., and Sacchettini, J. C. (1993) *Biochemistry 32*, 11963−11968.
28. Steinlein, L. M., Ligman, C. M., Kessler, S., and Ikeda, R. A. (1998) *Biochemistry 37*, 13696−13703.
29. He, Q.-Y., Mason, A. B., Tam, B. M., MacGillivray, R. T. A., and Woodworth, R. C. (1999) *Biochemistry 38*, 9704−9711.
30. Day, C. L., Stowell, K. M., Baker, E. N., and Tweedie, J. W. (1992) *J. Biol. Chem. 267*, 13857−13862.
31. Ward, P. P., Zhou, X., and Conneely, O. M. (1996) *J. Biol. Chem. 271*, 12790−12794.
32. Baker, E. N., and Lindley, P. F. (1992) *J. Inorg. Biochem. 47*, 147−160.
33. Baldwin, G. S. (1993) *Comp. Biochem. Physiol. 106B*, 203−218.
34. He, Q.-Y., Mason, A. B., Woodworth, R. C., Tam, B. M., MacGillivray, R. T. A., Grady, J. K., and Chasteen, N. D. (1998) *J. Biol. Chem. 273*, 17018−17024.

BI010907P